© 2026 Journal of Pharmacy & Pharmacognosy Research, 14 (2), 2415, 2026
ISSN 0719-4250
https://jppres.com

DOI: https://doi.org/10.56499/jppres_14.2.2415

Original Article

Neuroprotective effects of nanoformulated *Paraboea leuserensis* B.L.Burtt on memory loss and depression in traumatic brain injury–induced rats: Behavioral and molecular insights

[Efectos neuroprotectores de *Paraboea leuserensis* B.L.Burtt nanoformulada sobre la pérdida de memoria y la depresión en ratas con lesión cerebral traumática inducida: perspectivas conductuales y moleculares]

Syafruddin Ilyas[1*], Yurnadi Hanafi Midoen[2], Safni Safni[3]

[1]Study Program of Biology, Faculty of Mathematics and Natural Sciences, Universitas Sumatera Utara, Medan, Indonesia.
[2]Department of Medical Biology, Faculty of Medicine, Universitas Indonesia, Jakarta, Indonesia.
[3]Department of Chemistry, Faculty of Mathematics and Natural Sciences, Universitas Andalas, Padang, Indonesia.
*E-mail: syafruddin6@usu.ac.id

Abstract

Context: Traumatic brain injury (TBI) is a major neurological disorder leading to memory loss and depression due to neuroinflammation and neuronal damage.

Aims: To evaluate the neuroprotective effects of nanoformulated *Paraboea leuserensis* (PL) on behavioral and molecular alterations in TBI-induced rats.

Methods: Male rats were divided into six groups: CN (normal), CP (TBI), MP (TBI + methylprednisolone 2 mg/200 g), PL20 (TBI + PL 20 mg/200 g), PL40 (TBI + PL 40 mg/200 g), and PL60 (TBI + PL 60 mg/200 g). Behavioral tests assessed memory and anxiety/depression. Histopathology of the CA3 hippocampus was analyzed, while molecular markers included BDNF and serotonin (ELISA), and BDNF, IL-1β, and caspase-3 (IHC).

Results: TBI significantly impaired memory (p=0.031) and increased depressive-like behavior (p=0.045), accompanied by neuronal damage in CA3. PL40 and PL60 markedly improved behavioral performance (p<0.05), increased BDNF (PL40: +42%, p=0.022; PL60: +47%, p=0.018) and serotonin levels (PL40: +35%, p=0.029; PL60: +38%, p=0.026), while reducing IL-1β (PL40: –31%, p=0.033; PL60: –36%, p=0.027) and caspase-3 expression (PL40: –28%, p=0.041; PL60: –32%, p=0.038). MP showed similar effects but less consistency.

Conclusions: Nanoformulated PL exerted significant neuroprotective and anti-inflammatory effects in TBI-induced rats, with PL40 and PL60 providing the greatest benefit. These findings highlight PL as a promising alternative or adjunctive therapy for TBI.

Keywords: BDNF; hippocampus; nanoformulation; neuroprotection; *Paraboea leuserensis*; traumatic brain injury.

Resumen

Contexto: El traumatismo craneoencefálico (TCE) es un trastorno neurológico importante que provoca pérdida de memoria y depresión debido a la neuroinflamación y el daño neuronal.

Objetivos: Evaluar los efectos neuroprotectores de *Paraboea leuserensis* (PL) nanoformulada sobre las alteraciones conductuales y moleculares en ratas con TCE inducido.

Métodos: Las ratas machos se dividieron en seis grupos: CN (normal), CP (TCE), MP (TCE + metilprednisolona 2 mg/200 g), PL20 (TCE + PL 20 mg/200 g), PL40 (TCE + PL 40 mg/200 g) y PL60 (TCE + PL 60 mg/200 g). Las pruebas conductuales evaluaron la memoria y la ansiedad/depresión. Se analizó la histopatología del hipocampo CA3, mientras que los marcadores moleculares incluyeron BDNF y serotonina (ELISA), y BDNF, IL-1β y caspasa-3 (IHQ).

Resultados: El TCE afectó significativamente la memoria (p=0,031) y aumentó la conducta depresiva (p=0,045), acompañada de daño neuronal en CA3. PL40 y PL60 mejoraron notablemente el rendimiento conductual (p < 0,05), aumentaron los niveles de BDNF (PL40: +42%, p=0,022; PL60: +47%, p=0,018) y serotonina (PL40: +35 %, p=0,029; PL60: +38 %, p=0,026), mientras que redujeron la expresión de IL-1β (PL40: –31%, p=0,033; PL60: –36%, p=0,027) y caspasa-3 (PL40: –28%, p=0,041; PL60: –32%, p=0,038). La MP mostró efectos similares, pero menos consistentes.

Conclusiones: El PL nanoformulado ejerció efectos neuroprotectores y antiinflamatorios significativos en ratas con TCE inducido, siendo el PL40 y el PL60 los que proporcionaron el mayor beneficio. Estos hallazgos destacan al PL como una alternativa prometedora o terapia complementaria para el TCE.

Palabras Clave: BDNF; hipocampo; lesión cerebral traumática; nanoformulación; neuroprotección; *Paraboea leuserensis*.

ARTICLE INFO
Received: March 7, 2025.
Accepted: December 4, 2025.
Available Online: April 30, 2026.

AUTHOR INFO
ORCID:
0000-0003-2760-2901 (SI)
0000-0003-0307-5211 (SS)
0000-0003-1594-6475 (YHM)

Abbreviations: ANOVA: Analysis of Variance; BBB: Blood-Brain Barrier; BDNF: Brain-Derived Neurotrophic Factor; Caspase-3: Cysteine-aspartic acid protease 3; CREB: cAMP response element-binding protein; ELISA: Enzyme-linked immunosorbent assay; IHC: Immunohistochemistry; IL-1β: Interleukin-1 beta; MP: Methylprednisolone; NF-κB: Nuclear Factor kappa-light-chain-enhancer of activated B cells; PL: *Paraboea leuserensis*; ROS: Reactive Oxygen Species; SD: Standard Deviation; SEM: Standard Error of the Mean; TBI: Traumatic Brain Injury.

INTRODUCTION

Traumatic brain injury (TBI) remains a pressing worldwide health issue, often leading to persistent neurological complications such as cognitive impairment, depressive symptoms, and increased anxiety (Akamatsu & Hanafy, 2020; Aqel et al., 2024). The underlying pathology of TBI encompasses a breakdown of neural homeostasis, marked by neuroinflammation, oxidative stress, excitotoxicity, and programmed cell death, with the hippocampus identified as a particularly vulnerable structure (Browmick et al., 2019; Silvestro & Mazzon, 2023). The CA3 area of the hippocampus is notably susceptible to secondary damage due to its extensive synaptic inputs from the dentate gyrus and outputs to CA1. Impairment in CA3 has been linked to declines in learning and memory, emotional dysregulation, and the development of neurodegenerative conditions after TBI (Arjadi et al., 2014; Slomianka et al., 2011).

At a molecular level, TBI significantly dysregulates neurotrophic signaling and neurotransmitter systems, especially affecting brain-derived neurotrophic factor (BDNF) and serotonin (Majeed et al., 2023; Musi et al., 2020). These molecules are vital for synaptic plasticity, neuronal survival, and emotional control (Aqel et al., 2024; Majeed et al., 2023). Furthermore, pro-inflammatory cytokines like interleukin-1 beta (IL-1β) are instrumental in driving the neuroinflammatory cascade (Deng et al., 2022; Jeon et al., 2024), while apoptotic executors such as caspase-3 significantly contribute to neuronal damage (Abd El Salam et al., 2023; Bhowmick et al., 2019; Jana et al., 2014). Collectively, these alterations hasten neurodegeneration and underpin the psychiatric symptoms observed following TBI (Majeed et al., 2023; Musi et al., 2020).

Methylprednisolone (MP) is a commonly used anti-inflammatory agent for the management of TBI (Mehta et al., 2022). Nonetheless, debate surrounds its therapeutic benefits due to associated risks, such as immunosuppression, impaired healing, and increased infection rates. This underscores the urgent need for novel treatments that are both safer and more effective.

The emergence of nanotechnology in herbal medicine offers promising neuroprotective strategies for TBI. Nanoformulated PL, a flavonoid-rich botanical extract with strong antioxidant, anti-inflammatory, and neurotrophic activities, has demonstrated efficacy in preclinical models of neurodegeneration and psychiatric illness (Marbun & Suryanto, 2024; Wasnis et al., 2022). Its nano-encapsulation improves bioavailability, facilitates crossing biological barriers, and allows for targeted action, positioning it as a viable option for TBI treatment (Keating & Cullen, 2021; Mohammed et al., 2023). However, the capacity of nanoherbal PL to alleviate TBI-related cognitive and emotional deficits has not been investigated.

Although the potential of herbal medicine for neuroprotection is gaining increased attention, the existing literature is marked by several pivotal shortcomings. There is a notable scarcity of studies dedicated to exploring how nanoformulated herbal compounds, specifically in the context of TBI, can protect against memory loss and depression. Furthermore, evaluations of nanoherbal treatments in TBI models often fail to integrate comprehensive behavioral testing with molecular-level analyses (James et al., 2019; Wu et al., 2022). Another significant gap is the lack of robust comparative data comparing nanoherbal therapy with standard corticosteroid treatments such as Methylprednisolone, particularly regarding their efficacy in reducing neuroinflammation, preventing apoptosis, and restoring neurotransmitter balance (Ferrell, 2015; Mehta et al., 2022). Filling these research gaps is imperative for advancing effective, safe, and sustainable neuroprotective solutions for TBI-induced neuropsychiatric conditions.

The promise of nanoformulated PL as a therapeutic agent is rooted in its multifaceted capabilities. It is poised to offer superior neuroprotection by simultaneously attenuating oxidative stress and inflammatory responses. Concurrently, it promotes neuroplasticity by enhancing the expression of key signaling molecules, BDNF and serotonin. The compound also demonstrates the ability to curb programmed cell death by regulating critical mediators, such as caspase-3 and IL-1β. Perhaps most importantly, it offers a natural, biocompatible treatment strategy that avoids the detrimental side effects commonly associated with conventional corticosteroid regimens.

This study was designed to methodically assess the neuroprotective potential of nanoencapsulated *Paraboea leuserensis* (PL) in a rodent model of traumatic brain injury. The research strategy incorporated a comprehensive methodology, integrating behavioral analyses, histopathological examination, and molecular-level evaluations. Key objectives included: 1) the quantification of memory deficits and depression-like behaviors through validated behavioral paradigms; 2) the assessment of neuronal damage in the susceptible hippocampal CA3 area via hematoxylin-eosin (HE) staining, following established protocols (Midoen et

al., 2023), and 3) perform a detailed analysis of key biomarkers. This includes measuring BDNF and serotonin levels via ELISA (Ilyas et al., 2023; Shen et al., 2023) and visualizing the expression patterns of BDNF, IL-1β, and caspase-3 in the CA3 region of the hippocampus using immunohistochemistry (Ilyas et al., 2025; Yusuf et al., 2016). A central objective is to directly compare the therapeutic efficacy of three doses of nanoformulated PL (PL20, PL40, PL60) with methylprednisolone (MP).

It is anticipated that this research will yield essential insights into the value of nanoformulated PL for managing TBI. The findings could make substantial contributions to the field by paving the way for innovative nanoherbal treatments aimed at the cognitive and psychiatric consequences of TBI. This work also bridges the disciplines of nanomedicine and neuroprotection, potentially offering a safer, more effective alternative to corticosteroids. Ultimately, the study seeks to broaden the clinical applicability of natural compounds for the treatment of complex neurological and psychiatric disorders.

MATERIAL AND METHODS

Plant material and authentication

Fresh specimens of PL were collected from Namo Sialang and Sei Serdang, Batang Serangan Sub-District, Langkat District, North Sumatra, Indonesia (UTM coordinates: x = 395928.28, y = 408308.48). The plant material was taxonomically identified by researchers at the National Research and Innovation Agency (BRIN), Indonesia, and a voucher specimen was deposited with Registration No.: B-1216/11.6.2/ir.01.02/6/2023. The leaves were used to prepare the extract.

Preparation and characterization of nanoformulated PL

The nanoformulation of PL was produced using a High-Energy Milling (HEM) technique, following a previously reported procedure with minor modifications. The initial step involved washing and air-drying leaves, resulting in a dried plant material at room temperature for three days before grinding them into a fine powder. This powdered material was then nanosized using the HEM process. The powder was loaded into a milling jar, and milling balls of assorted varying diameters were added, ensuring the total volume did not exceed two-thirds of the jar's capacity. The sealed jar was then processed in the HEM apparatus for two hours. The resulting nanoformulation was collected and stored in a sealed container at room temperature for subsequent use in analysis (Situmorang et al., 2019).

Experimental design

A randomized, controlled laboratory paradigm was adopted for this investigation. Male Sprague-Dawley rats weighing 200–250 g were procured from an accredited supplier. The animals were housed in a controlled environment maintained at 22 ± 2°C, 55 ± 5% relative humidity, and a standardized 12-hour light/dark cycle. They had unrestricted access to a standard rodent diet and water. All experimental procedures were approved by the Institutional Animal Ethics Committee (Ethical Clearance No.: 0432/KEPH-FMIPA/2024) and strictly conformed to the ARRIVE guidelines as well as the National Institutes of Health (NIH) guidelines for animal experimentation (Bayne, 1996).

Animal grouping and treatment

Rats were randomly assigned to one of six experimental groups, with five animals per group. The groups were defined as follows: the Negative Control (CN) group consisted of healthy rats without TBI that received only the vehicle; the Positive Control (CP) group comprised TBI-induced rats that received no treatment; the MP group included TBI-induced rats treated with 2 mg/200 g body weight of MP via intraperitoneal injection; and the PL20, PL40, and PL60 groups contained TBI-induced rats administered nanoformulated PL at doses of 20, 40, and 60 mg/200 g body weight, respectively, via oral gavage. The basis for dose selection was derived from earlier work by Ashfira et al. (2024), which had employed doses of 100 mg/kg BW and 125 mg/kg BW, equivalent to 20 mg/200 g BW and 25 mg/200 g BW, respectively. Therefore, the 20 mg/200 g BW dose was chosen as the starting point, while the 40 and 60 mg/200 g BW doses were introduced as additional tiers to thoroughly evaluate the dose-response efficacy of the treatment.

Induction of TBI

TBI injury was induced in the rats via a standardized weight-drop impact technique. Briefly, animals were first anesthetized with ketamine. Subsequently, a 50-gram iron ball with a 4 mm diameter was dropped from a height of 2 meters onto the exposed skull to create the injury. The experimental cohort consisted of 30 rats, distributed across six groups of five animals each, as determined by Federer's formula $(t-1)(n-1)\geq 15$, where $t=6$ and $n=5$ (Kurniawan et al., 2022). To ensure the target sample size was achieved, an allowance was made for the potential exclusion of approximately 10% of the animals over the course of the experiment.

Treatment administration

Post-TBI induction, all therapeutic interventions were administered once daily for 30 consecutive days. The nanoformulated PL was prepared as a suspension in sterile distilled water and administered by oral gavage to the animals. In contrast, the MP was administered through an intraperitoneal injection. To serve as a vehicle control, the animals in the relevant control groups were given a comparable volume of sterile distilled water following the same schedule.

Behavioral assessments

Memory deficits and depression-like behaviors were evaluated using a series of validated tests, as detailed below.

Latency time (s) in the open field test (OFT)

Anxiety-like behavior was quantified in an open field arena (50 × 50 cm^2) by measuring latency. This parameter was defined as the duration, in seconds, required for a rat to transition from the central zone of the arena to a corner zone following placement (Akash et al., 2024).

Number of squares crossed in the OFT

Exploratory and anxiety-like behavior was also gauged through locomotor activity in the OFT, conducted after the 30-day intervention. Each rat was positioned in the center of a gridded arena (50 × 50 cm^2), and its movement was video recorded for 10 minutes. The total number of grid lines traversed was counted, where a lower count signifies reduced exploratory drive or heightened anxiety (Seibenhener & Wooten, 2015).

Rearing in the OFT

The OFT was further used to assess exploratory drive by documenting rearing behavior. This was characterized as the frequency with which a rat stood on its hind legs during the 10-minute trial, serving as an indicator of vertical exploration. A reduction in the number of rearing events was considered evidence of increased anxiety or decreased motivation to explore the environment (Seibenhener & Wooten, 2015).

Time spent in the OFT

Anxiety-like behavior was further evaluated in the OFT by quantifying the cumulative time spent in the arena's central zone during the 10-minute trial. A reduced time spent in this open, exposed area was considered a behavioral indicator of elevated anxiety.

Number of interactions in the social interaction test (SIT)

Depressive-like responses were evaluated after the 30-day treatment period using the SIT. The test was performed in a transparent arena under bright light conditions. Two rats from different groups, each marked with a distinctive non-toxic dye for identification, were placed together for a 10-minute session. Specific social behaviors, including sniffing, following, grooming, chasing, aggression, and climbing, were quantified. The cumulative time spent in active social interaction was recorded manually with a stopwatch and corroborated by video recording. A decrease in total interaction time was indicative of social withdrawal, a core depressive-like symptom (Shahzad et al., 2017; Thanos et al., 2017).

Analysis of memory impairment associated with depression in rats (Recognition Index)

Memory impairment related to depressive-like behavior was evaluated on day 30 of treatment using the Pattern Separation Test (PST). This paradigm assesses spatial recognition memory by measuring a rat's ability to distinguish between objects following positional changes (Chang et al., 2024). Testing was conducted in a square arena housed within a sound-attenuated room under bright white lighting. Prior to each trial, the apparatus was meticulously cleaned with a 70% ethanol solution to eliminate residual olfactory cues that could influence behavior.

The PST protocol comprised two sequential phases: training and testing. In the initial training phase, individual rats were positioned in the arena's center for a 5-minute session with two identical objects (designated A and B) arranged in parallel. Following this acquisition period, animals returned to their home cages for a 20-minute retention interval. During the subsequent testing phase, rats were re-exposed to the arena for 5 minutes, during which object A remained in its original position, while object B was relocated to a novel location. Object exploration was quantitatively defined as the cumulative time spent actively sniffing or directing the nose toward an object within a 2 cm proximity. The key outcome measure was the Recognition Index (RI), determined using the following formula [1]:

$$B / (A + B) = IR \quad [1]$$

Where A: time spent sniffing an object that remained in position during the training session and testing session; B: time spent sniffing an object that moved its position during the testing session (Mathiasen & Dicamillo, 2010).

Histopathological analysis

Following the final behavioral assessments, rats were deeply anesthetized and followed by transcardial

perfusion with 4% paraformaldehyde. The brain tissue was subsequently carefully extracted, and 5 µm-thick coronal sections containing the hippocampal CA3 area were prepared. For histological evaluation, these sections were stained with hematoxylin and eosin to assess neuronal structure, degenerative changes, inflammatory infiltration, and overall tissue integrity (Akamatsu & Hanafy, 2020). Observation was performed under light microscopy, and representative digital images were captured for qualitative analysis.

Molecular analysis

Enzyme-linked immunosorbent assay (ELISA)

Hippocampal tissue homogenates were analyzed for BDNF and serotonin levels using commercially available ELISA kits (Abcam, USA; Catalog Nos. ab213899 and ab133053), with all procedures conducted according to the manufacturer's specifications. Absorbance was measured at a wavelength of 450 nm using a BioTek microplate reader (USA). Final analyte concentrations were determined through interpolation from standard curves established for each target molecule.

Immunohistochemistry (IHC) analysis

Protein expression levels of BDNF, IL-1β, and caspase-3 in the hippocampal CA3 area were visualized via immunohistochemistry. Following a standard protocol, tissue sections were incubated with specific primary antibodies (diluted 1:500) overnight at 4°C. This was followed by incubation with HRP-conjugated secondary antibodies. A DAB substrate was used to develop chromogenic signals, and hematoxylin was applied as a nuclear counterstain. After dehydration and mounting, images were acquired with an Olympus BX53 microscope. A semi-quantitative analysis of immunoreactive staining density was subsequently performed using ImageJ software.

Statistical analysis

Data analysis was conducted using GraphPad Prism software (version 9.0, USA). Values are reported as mean ± SEM. Validation of parametric test assumptions was performed by assessing normality with the Shapiro-Wilk test and verifying variance homogeneity with Levene's test. Inter-group comparisons were evaluated using a one-way ANOVA followed by Tukey's *post hoc* test. Longitudinal behavioral data were subjected to repeated-measures ANOVA. Statistical significance was defined as $p<0.05$ for all analyses.

RESULTS

Locomotor activity parameters

The impact of various therapeutic interventions on locomotor function was assessed by measuring latency time in a rodent model of TBI, as detailed in Fig. 1A. Rats in the CN group, which were healthy and untreated, demonstrated a baseline latency period. Conversely, the CP group, comprising TBI-induced rats that received no therapy, showed a statistically significant prolongation of latency compared with the CN group ($p<0.0001$). Treatment with MP at a dose of 2 mg/200 g body weight decreased latency time compared with the CP group; however, these values remained elevated above the CN baseline.

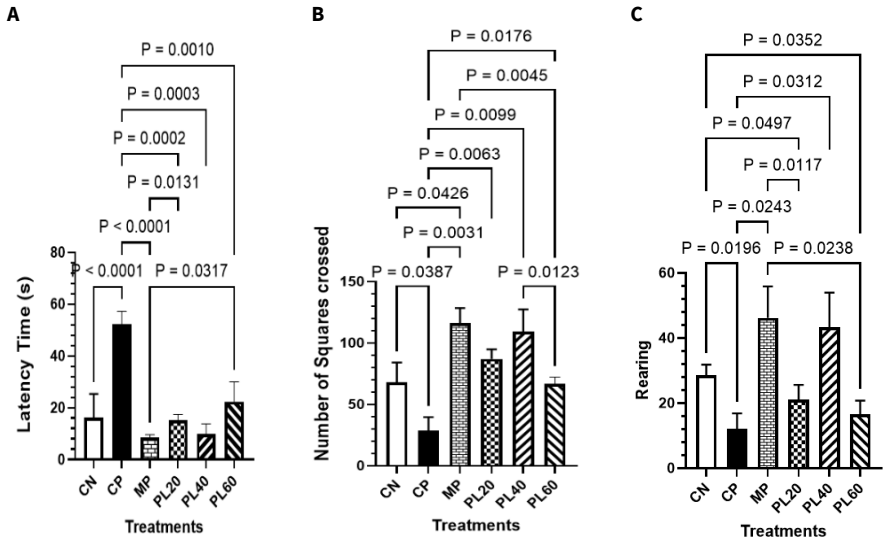

Figure 1. Locomotor activity parameters.

(A) Latency time (s): The delay time before the subject starts moving or responding to a stimulus. **(B)** Number of squares crossed: The number of squares crossed in the test arena, indicating locomotor activity levels. **(C)** Rearing: The frequency of the subject standing on its hind legs, often used to assess exploration and vertical motor activity.

Data from three bar graphs are expressed as mean + SD. The results showing the number of "P" in all graphs are significantly different by ANOVA followed by a Tukey's test ($p\leq0.05$). CN (Negative Control): Normal, untreated rats. CP (Positive Control): Traumatic brain injury (TBI)-induced rats without treatment. MP: TBI-induced rats treated with 2 mg/200 g methylprednisolone. PL20: TBI-induced rats treated with nanoformulated *Paraboea leuserensis* (20 mg/200 g body weight). PL40: TBI-induced rats treated with nanoformulated *Paraboea leuserensis* (40 mg/200 g body weight). PL60: TBI-induced rats treated with nanoformulated *Paraboea leuserensis* (60 mg/200 g body weight).

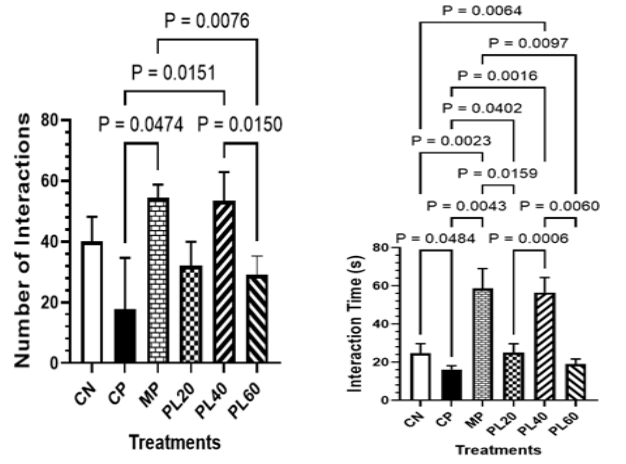

Figure 2. Social interaction parameters.

(A) Number of interactions: The number of interactions the subject has with another object or individual in the test environment. **(B)** Interaction time (s): The total duration spent interacting with an object or another subject.

Data from three bar graphs are expressed as mean + SD. The results showing the number of "P" in all graphs are significantly different by ANOVA followed by a Tukey's test ($p \leq 0.05$). CN (Negative Control): Normal, untreated rats. CP (Positive Control): Traumatic brain injury (TBI)-induced rats without treatment. MP: TBI-induced rats treated with 2 mg/200 g methylprednisolone. PL20: TBI-induced rats treated with nanoformulated *Paraboea leuserensis* (20 mg/200 g body weight). PL40: TBI-induced rats treated with nanoformulated *Paraboea leuserensis* (40 mg/200 g body weight). PL60: TBI-induced rats treated with nanoformulated *Paraboea leuserensis* (60 mg/200 g body weight).

Intervention with nanoformulated PL also ameliorated the TBI-induced deficit, as evidenced by reduced latency times across all tested doses (20, 40, and 60 mg/200 g BW) when compared to the CP group. The intermediate dose, PL40, induced a statistically significant reversal of the latency increase (p=0.0317) compared to the untreated TBI controls. This pattern of results indicates that PL exerts a neuroprotective effect on locomotor activity in a dose-responsive manner, with moderate and higher doses appearing more effective. A comprehensive evaluation of PL's efficacy requires its direct comparison with the standard treatment, MP.

As depicted in Fig. 1B, induction of TBI led to a substantial decline in motor function, evidenced by a significantly lower number of boxes crossed in the CP group relative to the CN. MP administration partially restored motor activity. Notably, treatment with the 40 mg/200 g dose of nanoformulated PL40 induced a more marked recovery than MP, a difference that was statistically significant (p=0.0063). No further enhancement was observed at the highest dose (PL60), suggesting that PL40 may be the most effective dose under the present experimental conditions.

The effect on exploratory behavior, measured by rearing frequency, is presented in Fig. 1C. TBI induction resulted in a significant decrease in rearing compared to the CN group (p=0.0196). While MP treatment successfully increased rearing frequency relative to the CP group (p=0.0243), the PL40 treatment again showed the most prominent effect. The improvement with PL40 was significant compared with the CP group (p=0.0117) and superior to the lower PL20 dose (p=0.0312). Consistent with the locomotor data, the PL60 dose did not confer benefits beyond those of PL40. Together, these findings indicate that nanoformulated PL at the 40 mg/200 g dose exhibited significant efficacy in countering TBI-induced motor and exploratory deficits, demonstrating effects comparable to, and in certain aspects surpassing, those of standard MP treatment.

Social interaction parameters

The effects on social behavior are presented in Fig. 2A-B. Induction of TBI resulted in a marked deficit in social behavior, characterized by statistically significant reductions in both interaction frequency (p=0.0474) and total interaction duration (p=0.0484) compared to the CN group. Treatment with MP effectively reversed these social deficits, affirming its therapeutic benefit. A similar restorative trend was observed in rats treated with nanoformulated PL. Among the PL-treated groups, the intermediate dose of 40 mg/200 g (PL40) elicited the greatest recovery, significantly enhancing both interaction frequency (p=0.0150 vs. CP; p=0.0151 vs. PL20) and duration (p=0.0006 vs. CP; p=0.0060 vs. PL20). The efficacy of PL40 was notably greater than that of the lower dose (PL20) and approached the level of improvement seen with MP. In contrast, the highest dose (PL60) showed a slight reduction in effect compared to PL40, indicating a potential non-linear, inverted U-shaped dose-response relationship for PL.

As detailed in Table 1, the quantitative data further substantiate these observations. The frequency of social interactions was 22 ± 1.2 in the CN group, which dropped significantly to 13.6 ± 1.6 in the CP group (p=0.0474). Similarly, interaction duration decreased from 24.6 ± 1.0 seconds in the CN group to 16.14 ± 0.4 seconds in the CP group (p=0.0484). MP treatment robustly increased these values (frequency: 53.2 ± 1.7; duration: 58.66 ± 2.1; $p<0.05$ vs. CP). The PL40 group demonstrated the most pronounced effect among the PL doses, with a frequency of 49.2 ± 2.0 and a duration of 56.54 ± 1.6, and showed significant improvement compared with both the CP group and the PL20 group. Although the PL60 group (frequency: 15.2 ± 0.5; duration: 18.94 ± 0.5) showed a modest decline relative to

PL40, its values remained superior to those of the untreated CP group. These collective results strongly suggest that the 40 mg/200 g dose of nanoformulated PL is the most effective for rescuing TBI-induced impairments in social behavior.

Exploration and cognitive performance parameters

Assessment of anxiety-related behavior and exploration was conducted by quantifying the time animals remained in the test zone (Fig. 3A). The TBI-induced CP group showed a significantly prolonged duration in the test zone relative to the normal CN group (p=0.0170), indicative of heightened anxiety or disrupted exploratory drive. This behavioral alteration was mitigated by treatment with both MP and nanoformulated PL across all tested doses. The most substantial anxiolytic effect was observed in the PL40 group, which showed a statistically significant reduction in test zone time relative to both the CP group (p=0.0097) and the PL20 group (p=0.0442). The lack of further improvement with the PL60 dose suggests that 40 mg/200 g body weight is the optimally effective dose for alleviating these anxiety-related behaviors post-TBI.

Cognitive performance, assessed via the recognition index, is shown in Fig. 3B. The CP group showed significant cognitive impairment, with a markedly lower recognition index than the CN group (p=0.0036). Both MP and nanoformulated PL treatments improved this metric. The PL40 dose again yielded the most prominent cognitive recovery, resulting in a significant increase in the recognition index compared with the CP group (p=0.0098). Notably, the efficacy of PL40 in restoring cognitive function surpassed that of the standard MP treatment (p=0.0105). Consistent with previous findings, the PL60 dose did not provide a superior effect compared with PL40, reinforcing that the 40 mg/200 g dose is optimal for enhancing memory and spatial recognition. These collective outcomes position nanoformulated PL, particularly at the 40 mg/200 g dose, as a promising therapeutic agent for addressing cognitive deficits following traumatic brain injury.

Table 1. Effect of *Paraboea leuserensis* (PL) nanoformulation on social interaction frequency and duration in the traumatic brain injury (TBI) rat model.

Group	Social interaction frequency (mean ± SEM)	Social interaction time (s, mean ± SEM)
CN	22 ± 1.2	24.6 ± 1.0
CP	13.6 ± 1.6	16.14 ± 0.4
MP	53.2 ± 1.7	58.66 ± 2.1
PL20	16 ± 0.6	25.04 ± 0.9
PL40	49.2 ± 2.0	56.54 ± 1.6
PL60	15.2 ± 0.5	18.94 ± 0.5

CN: Negative Control; CP: Positive Control, TBI; MP: Methylprednisolone; PL20: 20 mg/200 g; PL40: 40 mg/200 g; PL60: 60 mg/200 g.

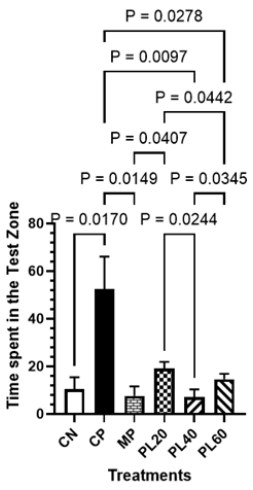

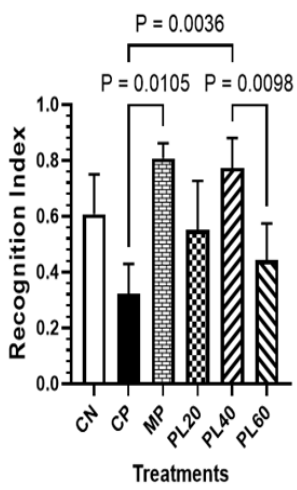

Figure 3. Exploration and cognitive performance parameters.

(A) Time spent in the test zone: The amount of time the subject spends in a specific zone within the test arena, which may indicate preference, anxiety levels, or exploratory interest. **(B)** Recognition index: A ratio or score measuring the subject's ability to recognize a novel object or individual compared to a familiar one, commonly used in memory and novel object recognition tests.

Data from three bar graphs are expressed as mean + SD. The results showing the number of "P" in all graphs are significantly different by ANOVA followed by a Tukey's test (p≤0.05). CN (Negative Control): Normal, untreated rats. CP (Positive Control): Traumatic brain injury (TBI)-induced rats without treatment. MP: TBI-induced rats treated with 2 mg/200 g methylprednisolone. PL20: TBI-induced rats treated with nanoformulated *Paraboea leuserensis* (20 mg/200 g body weight). PL40: TBI-induced rats treated with nanoformulated *Paraboea leuserensis* (40 mg/200 g body weight). PL60: TBI-induced rats treated with nanoformulated *Paraboea leuserensis* (60 mg/200 g body weight).

Hippocampal CA3 network in a model of traumatic brain injury

Histological assessment of the hippocampal CA3 area, shown in Fig. 4A-B, revealed extensive neurodegeneration following TBI induction. This neuronal injury manifested as a marked increase in pyknotic cells among CA3 pyramidal neurons, characterized by distinctive nuclear condensation indicative of apoptotic cell death. The CP group, which received TBI but no therapeutic intervention, exhibited the most severe level of pyknotic neurons, a finding that was statistically significant compared to the healthy CN group ($p=0.0005$) and confirmed extensive hippocampal degeneration. Intervention with both MP and nanoformulated PL resulted in a marked reduction of this neuronal damage relative to the untreated CP group. The neuroprotective efficacy was most pronounced with the PL40 dose, which showed a significant decrease in pyknosis compared with the CP group ($p=0.0024$). Notably, the protective effect appeared to diminish at the highest dose, as the PL60 group showed a modest increase in pyknotic cells compared to PL40. This pattern reinforces that the 40 mg/200 g dose is likely the optimal concentration for preserving neuronal integrity in the hippocampal CA3 network after a traumatic insult.

BDNF CA3 hippocampal expression in the traumatic brain injury model

Immunohistochemical examination of BDNF distribution in the CA3 hippocampal sector demonstrated notable differences among treatment cohorts, as illustrated in Fig. 5A-B. The CN group displayed abundant BDNF-immunopositive neurons. Conversely, TBI-induced CP animals without therapeutic intervention exhibited a significant reduction in BDNF-expressing cells, indicating compromised neurotrophic signaling after injury. These findings suggest that nanoformulated PL, particularly at the 40 mg/200 g dose, may enhance neurotrophic support in the hippocampal CA3 region, thereby contributing to neuronal survival and functional recovery following TBI. Therapeutic administration of MP and nanoformulated PL at all tested doses led to a notable recovery of BDNF immunoreactivity. The most robust upregulation of BDNF expression was achieved in the PL40 treatment group. Statistical comparisons confirmed that the increases in BDNF expression in both the MP and PL40 groups were statistically significant relative to the untreated CP group ($p<0.05$). Furthermore, the effect of the PL40 dose was more pronounced than that of the lower PL20 dose, hinting at a dose-responsive relationship. These results imply that nanoformulated PL, especially at the 40 mg/200 g dosage, can reinforce neurotrophic signaling in the hippocampus after TBI, a mechanism that likely supports neuronal repair and functional rehabilitation.

Caspase-3 expression in CA3 hippocampal neurons of the traumatic brain injury model

Representative immunohistochemical results for caspase-3 in the CA3 hippocampal area are shown in Fig. 6A-B. Traumatic brain injury induction led to a substantial increase in caspase-3 immunoreactivity, indicating enhanced activation of apoptotic mechanisms. Statistical analysis verified significantly higher caspase-3 expression in the CP group compared to the CN group ($p=0.0014$). MP administration effectively reduced this apoptotic response ($p=0.0043$ vs CP), confirming its anti-apoptotic efficacy.

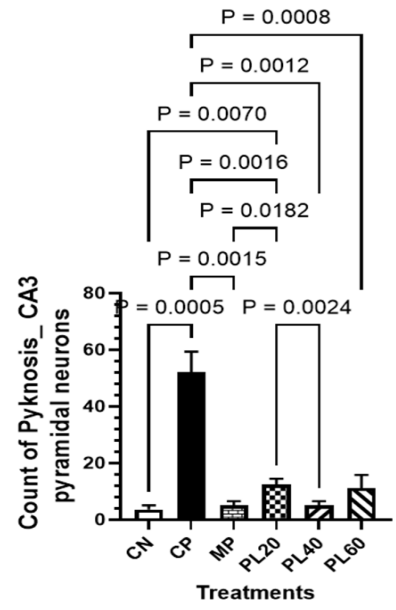

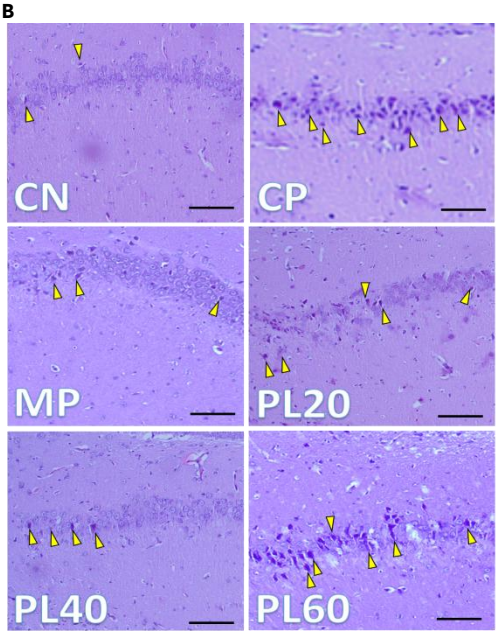

Figure 4. (A) Count of Pyknosis_CA3. **(B)** Histology of CA3 hippocampus in TBI model rats.

Data from bar graphs are expressed as mean ± SD. Statistical differences were analyzed using one-way ANOVA followed by Tukey's post hoc test ($p\leq0.05$). CN (Negative Control): Normal, untreated rats. CP (Positive Control): Traumatic brain injury (TBI)-induced rats without treatment; MP: Methylprednisolone, 2 mg/200 g BW, i.p.; PL20: Nanoformulated *Paraboea leuserensis*, 20 mg/200 g BW, oral); PL40: Nanoformulated *Paraboea leuserensis*, 40 mg/200 g BW, oral; PL60: Nanoformulated *Paraboea leuserensis*, 60 mg/200 g BW, oral.

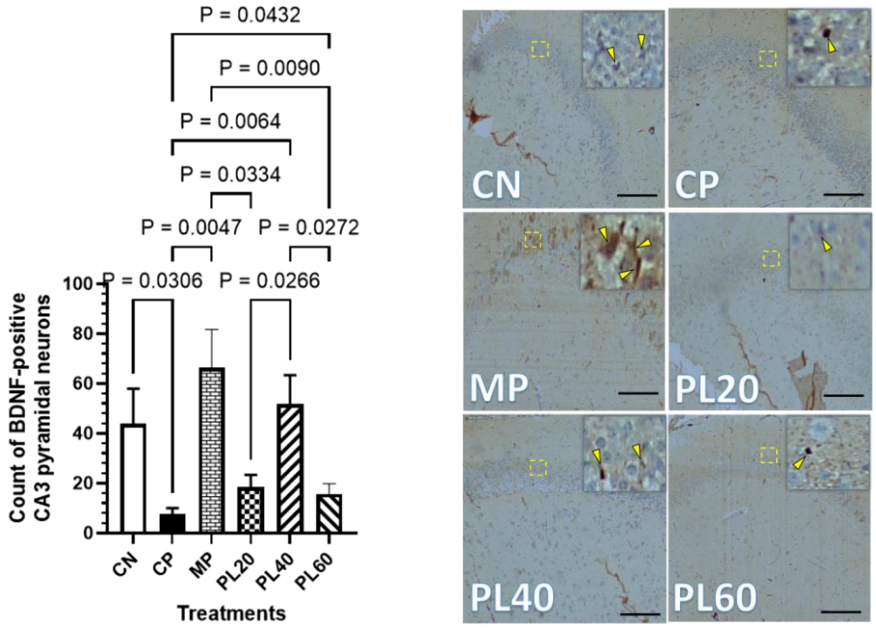

Figure 5. (A) Count of BDNF-positive CA3 pyramidal neurons. **(B)** Expression of BDNF in hippocampal tissue of the TBI model by immunohistochemistry.

Data from three bar graphs are expressed as mean + SD. The results showing the number of "P" in all graphs are significantly different by ANOVA followed by a Tukey's test (p≤0.05). CN (Negative Control): Normal, untreated rats. CP (Positive Control): Traumatic brain injury (TBI)-induced rats without treatment. MP: TBI-induced rats treated with 2 mg/200 g methylprednisolone. PL20: TBI-induced rats treated with nanoformulated *Paraboea leuserensis* (20 mg/200 g body weight). PL40: TBI-induced rats treated with nanoformulated *Paraboea leuserensis* (40 mg/200 g body weight). PL60: TBI-induced rats treated with nanoformulated *Paraboea leuserensis* (60 mg/200 g body weight).

In cohorts receiving nanoformulated PL, the intermediate dose of 40 mg/200 g (PL40) produced the greatest suppression of caspase-3, evidenced by a highly significant reduction compared with the CP group (p=0.0013). The lower (PL20) and higher (PL60) doses also conferred significant protective effects against apoptosis (p=0.0100 and p=0.0041 vs. CP, respectively). Importantly, the PL40 intervention was statistically superior to both the PL20 (p=0.0362) and PL60 (p=0.0493) groups. This pattern confirms that the 40 mg/200 g dose is optimal for countering apoptosis.

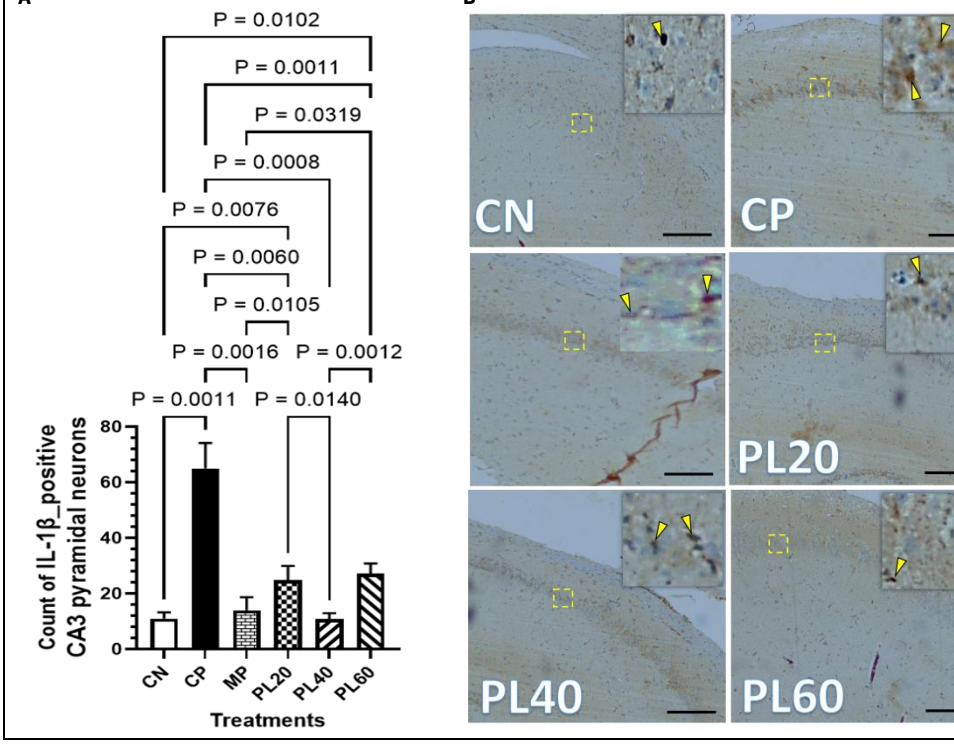

Figure 6. (A) Count of IL-1β positive CA3 pyramidal neurons. **(B)** Expression of IL-1β in hippocampal tissue of the TBI model by IHC.

Data from three bar graphs are expressed as mean + SD. The results showing the number of "P" in all graphs are significantly different by ANOVA followed by a Tukey's test (p≤0.05). CN (Negative Control): Normal, untreated rats. CP (Positive Control): Traumatic brain injury (TBI)-induced rats without treatment. MP: TBI-induced rats treated with 2 mg/200 g methylprednisolone. PL20: TBI-induced rats treated with nanoformulated *Paraboea leuserensis* (20 mg/200 g body weight). PL40: TBI-induced rats treated with nanoformulated *Paraboea leuserensis* (40 mg/200 g body weight). PL60: TBI-induced rats treated with nanoformulated *Paraboea leuserensis* (60 mg/200 g body weight).

In summary, these data demonstrate that nanoformulated PL, specifically at the 40 mg/200 g dose, is a potent inhibitor of apoptosis in the hippocampal CA3 region following TBI, with efficacy comparable to that of the standard MP therapy.

Caspase-3 expression in the hippocampal CA3 region of the traumatic brain injury model

Quantitative analysis confirmed a significant escalation in apoptotic activity within the hippocampal CA3 region following TBI, as evidenced by a markedly higher count of caspase-3-positive neurons in the CP group compared to the CN group ($p=0.0014$). Therapeutic intervention with MP effectively counteracted this effect, resulting in a significant reduction in caspase-3 expression compared with the CP group ($p=0.0043$).

Among the nanoformulated PL treatment groups, a dose-dependent modulation of this apoptotic marker was observed. The PL40 dose (40 mg/200 g BW) was the most potent, demonstrating highly significant suppression of caspase-3 ($p=0.0013$ vs. CP). While the PL20 and PL60 doses also produced significant anti-apoptotic effects ($p=0.0100$ and $p=0.0041$ vs. CP, respectively), their efficacy was inferior to that of PL40. This was statistically confirmed by direct comparisons showing that PL40 was significantly more effective than both PL20 ($p=0.0362$) and PL60 ($p=0.0493$). The attenuated effect at the highest dose (PL60) suggests a potential saturation or decline in efficacy beyond the optimal concentration. Collectively, these findings establish that nanoformulated PL at a dose of 40 mg/200 g body weight was a highly effective agent for inhibiting TBI-induced neuronal apoptosis in the CA3 hippocampus, with potency comparable to standard MP therapy (Fig. 7).

DISCUSSION

This investigation provides compelling evidence that nanoformulated PL offers significant neuroprotective benefits in a TBI model, primarily by attenuating neuroinflammatory cascades, suppressing apoptotic activity, and enhancing neuroplasticity. Consistent with the literature, the pathological CP group showed a substantial upregulation of IL-1β, indicative of pronounced microglial activation and dysregulated neuroinflammation post-TBI (Mohammed et al., 2023). IL-1β is a well-characterized driver of secondary injury, known to amplify neuronal degeneration and underpin associated cognitive and affective deficits (Deng et al., 2022). Our results identify the 40 mg/200 g BW dose of PL (PL40) as the most effective in curtailing IL-1β expression, surpassing the effects of both lower (PL20) and higher (PL60) doses. This dose-response profile posits PL40 as the optimal therapeutic window. The anti-inflammatory efficacy of PL40 is consistent with prior studies showing that flavonoid-rich extracts can inhibit the NF-κB pathway, leading to downregulation of pro-inflammatory cytokines such as IL-1β (Adeyi et al., 2023).

Concurrent with neuroinflammation, TBI triggered significant apoptotic cell death in the hippocampal CA3 region, as demonstrated by elevated caspase-3 expression. This underscores the contribution of the intrinsic apoptotic pathway to TBI-related neuronal loss (Slomianka et al., 2011). The CP group showed a marked increase in caspase-3-positive neurons compared to the CN, validating apoptosis as a key mechanism of post-TBI degeneration. Both PL40 and MP treatments significantly reduced caspase-3 expression, demonstrating anti-apoptotic potency for PL comparable to that of conventional steroid therapy. It is noteworthy that while MP is clinically used, its utility is limited by side effects such as immunosuppression. In contrast, PL presents a potentially safer profile, with its neuroprotective effects likely derived from its natural antioxidant and anti-inflammatory constituents (Wang et al., 2021).

Furthermore, this study highlights the involvement of neuroplasticity in TBI recovery, illustrated by changes in BDNF expression. BDNF, a crucial regulator of synaptic integrity and cognitive function, was significantly depleted in the CP group, indicating a breakdown of plasticity mechanisms essential for recovery. Treatment with PL40 and PL60, however, significantly restored BDNF levels compared to the CP group, implying that nanoformulated PL facilitates neuronal repair by engaging plasticity-promoting pathways. This effect may be mediated through the cAMP response element-binding protein (CREB) signaling cascade, a known regulator of BDNF transcription (Chidambaram et al., 2024). The observed BDNF upregulation in PL-treated groups corresponded with enhanced cognitive performance in the PST, with the PL40 and PL60 groups showing superior recognition indices and spatial learning. This correlation between hippocampal BDNF recovery and cognitive improvement (Musi et al., 2020; Sai Kumar et al., 2023) strengthens the proposition that the neurotrophic action of PL is instrumental in rescuing memory functions compromised by TBI.

The therapeutic influence of nanoformulated PL extended to behavioral domains, notably mitigating anxiety and depression-like phenotypes observed post-TBI. In the OFT, rats subjected to TBI (CP group) displayed diminished exploratory drive and heightened passive coping strategies.

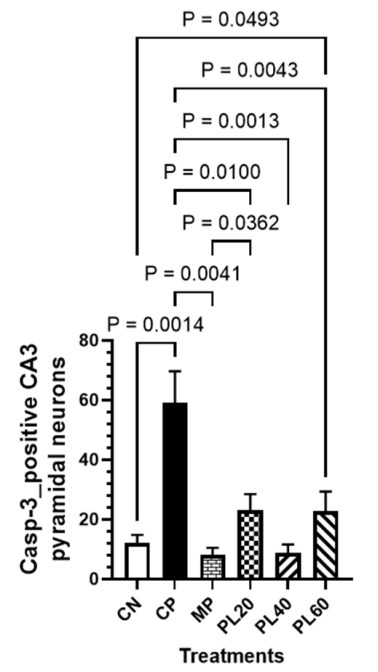

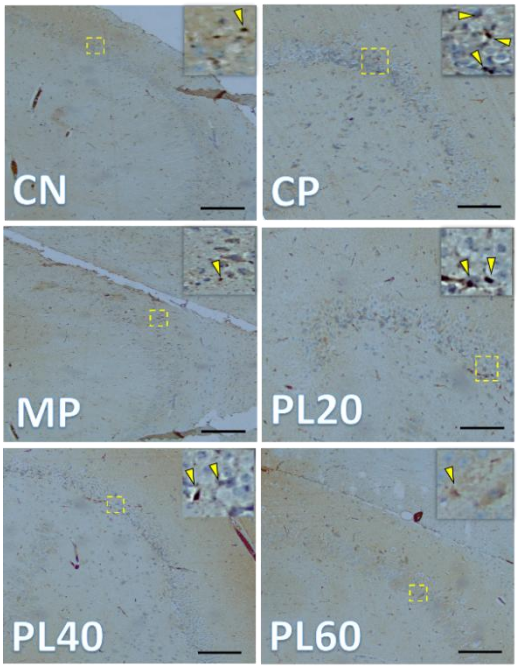

Figure 7. Count of caspase 3 positive CA3 pyramidal neurons. (B) Expression of caspase 3 in hippocampal tissue of the TBI model by IHC. Data from three bar graphs are expressed as mean + SD. The results showing the number of "P" in all graphs are significantly different by ANOVA followed by a Tukey's test ($p \leq 0.05$). CN (Negative Control): Normal, untreated rats. CP (Positive Control): Traumatic brain injury (TBI)-induced rats without treatment. MP: TBI-induced rats treated with 2 mg/200 g methylprednisolone. PL20: TBI-induced rats treated with nanoformulated *Paraboea leuserensis* (20 mg/200 g body weight). PL40: TBI-induced rats treated with nanoformulated *Paraboea leuserensis* (40 mg/200 g body weight). PL60: TBI-induced rats treated with nanoformulated *Paraboea leuserensis* (60 mg/200 g body weight).

Administration of the PL40 dose significantly counteracted these behavioral deficits, promoting exploratory activity and reducing immobility, which points to inherent anxiolytic and antidepressant properties. These positive behavioral shifts are likely mediated by the PL-induced upregulation of hippocampal BDNF and serotonin, both established as pivotal modulators of emotional states and affective responses (Agbolou et al., 2023). Consequently, the neuroprotective benefits of PL appear to translate into comprehensive functional recovery, encompassing both cognitive performance and emotional regulation.

A key finding of this investigation is the identification of PL40 as the optimally effective dose, outperforming both the lower (PL20) and higher (PL60) concentrations. The suboptimal response at the PL20 dose may be due to an inability to achieve the required therapeutic threshold in the target tissue. Conversely, the diminished returns at the PL60 dose could stem from pharmacokinetic limitations, such as receptor saturation or an accelerated clearance rate at elevated concentrations. This bell-shaped dose-response curve is a recognized phenomenon in nanoherbal therapeutics, where intermediate doses often yield maximal efficacy (Alqahtani et al., 2024; Majeed et al., 2023). Furthermore, the plateau in therapeutic benefit at higher doses might be explained by downregulation of neurotrophic receptors, in which BDNF levels exceed an optimal range, thereby blunting signaling necessary for neuroplasticity.

In summary, the collective data underscore the substantial neuroprotective capacity of nanoformulated PL in countering the multifaceted pathophysiology of TBI. The treatment effectively attenuated neuroinflammation, suppressed apoptotic cascades, and potentiated neuroplasticity, culminating in the preservation of neuronal integrity and the restoration of cognitive and affective functions. These outcomes illustrate the pleiotropic nature of PL, where molecular, cellular, and behavioral recoveries are intrinsically linked (Akamatsu & Hanafy, 2020; Mohammed et al., 2023). When compared to the standard corticosteroid Methylprednisolone, PL emerges as a compelling natural alternative, offering similar neuroprotective efficacy while potentially circumventing the adverse effects associated with long-term steroid use. These findings advocate for the further development of PL as a promising therapeutic candidate, either as a standalone or adjunctive treatment, for traumatic brain injury and potentially other conditions characterized by neurodegeneration and neuropsychiatric impairment. However, additional studies, including clinical validation and mechanistic investigations, are required to confirm these findings.

CONCLUSION

This study establishes that nanoformulated PL provides substantial neuroprotection in a TBI model, primarily by attenuating neuroinflammatory responses, inhibiting apoptotic pathways, and potentiating neuroplastic mechanisms. The intermediate dose of 40 mg/200 g BW (PL40) proved to be the most therapeutically effective, consistently outperforming other

doses. This optimal efficacy was evidenced by a significant downregulation of pro-inflammatory IL-1β and pro-apoptotic caspase-3, coupled with a marked upregulation of BDNF. These favorable molecular changes were directly correlated with enhanced performance in cognitive tests and the amelioration of anxiety and depression-like behaviors. When compared with methylprednisolone, PL may represent a promising natural alternative, leveraging its rich flavonoid and antioxidant profile to provide neuroprotection without the risks of systemic adverse effects. The collective findings positive of PL40 as the optimal dosage and nanoformulated PL as a highly promising candidate for complementary or alternative treatment strategies in traumatic brain injury and potentially other neurodegenerative conditions.

CONFLICT OF INTEREST

The research was conducted entirely free from any involvement in commercial, financial, or personal matters that might be perceived as a possible conflict of interest or that could have influenced the outcomes or interpretation of the study.

ACKNOWLEDGMENTS

This research was financially supported by the Riset Kolaborasi Indonesia (RKI) program, Universitas Sumatera Utara, Medan (No. 02/UN5.4.10.K/PPM/KP-RKI/2024); Universitas Indonesia, Jakarta (No. NKB-768/UN2.RST/HKP.05.00/2024); and Universitas Andalas, Padang (No. 25/UN16.19/PT.01.03/RKI/2024).

GENERATIVE ARTIFICIAL INTELLIGENCE (AI)

The authors used ChatGPT (OpenAI) to improve the language and readability of the manuscript. The authors reviewed and edited the content and take full responsibility for its accuracy. No images were generated or manipulated using AI tools.

REFERENCES

Abd El Salam ASG, Samaha MM, Abd Elrazik NA (2023) Cytoprotective effects of cinnamaldehyde and adipoRon against cyclophosphamide-induced cardio-renal toxicity in rats: Insights into oxidative stress, inflammation, and apoptosis. Int Immunopharmacol 124(Part B): 111044. https://doi.org/10.1016/j.intimp.2023.111044

Adeyi OE, Somade OT, Ajayi BO, James AS, Adeboye TR, Olufemi DA, Oyinlola EV, Sanyaolu ET, Mufutau IO (2023) The anti-inflammatory effect of ferulic acid is via the modulation of NFκB-TNF-α-IL-6 and STAT1-PIAS1 signaling pathways in 2-methoxyethanol-induced testicular inflammation in rats. Phytomedicine Plus 3(3): 100464. https://doi.org/10.1016/j.phyplu.2023.100464

Agbolou XM, Yoe CW, Cominski TP, Zimering MB (2023) Effects of a serotonin receptor peptide on behavioral pattern separation in sham- vs. mild traumatic brain injured rats. Endocrinol Diabetes Metab J 8(2): 10.31038/edmj.2024821. https://doi.org/10.31038/edmj.2024821

Akamatsu Y, Hanafy KA (2020) Cell death and recovery in traumatic brain injury. Neurotherapeutics 17(2): 446–456. https://doi.org/10.1007/s13311-020-00840-7

Akash A, Rani R, Singh AP, Singh AP (2024) Animals use to find anxiolytic activity: an updated review with advantage of each model. J Drug Deliv Ther 14(3): 210–217. https://doi.org/10.22270/jddt.v14i3.6488

Alqahtani F, Mohamed Ali YS, Almutairi MM, Alotaibi AF, Imran I, Alshammari MA, Alshememry AK, AlSharari SD, Albekairi TH (2024) Therapeutic benefits of quercetin in traumatic brain injury model exposed to cigarette smoke. Saudi Pharm J 32(1): 101895. https://doi.org/10.1016/j.jsps.2023.101895

Aqel S, Al-Thani N, Haider MZ, Abdelhady S, Al Thani AA, Kobeissy F, Shaito AA (2024) Biomaterials in traumatic brain injury: perspectives and challenges. Biology 13(1): 21. https://doi.org/10.3390/biology13010021

Arjadi F, Soejono SK, Maurits LS, Pangestu M (2014) Number of CA3 pyramidal cell in male albino rat hippocampus exposed to various chronic work stress models. J Anat Kedokteran Indonesia 46(4): 197–202. http://dx.doi.org/10.15395/mkb.v46n4.337

Ashfira, Ilyas S, Tanjung M (2024) Expression of caspase 3 in rat liver cells by maximum physical exercise after administration of gagatan harimau nanoherbal (*Paraboea leuserensis* B.L.Burtt). Biovalentia Biol Res J 9(2): 162–167. https://doi.org/10.24233/biov.9.2.2023.411

Bayne K (1996) Revised guide for the care and use of laboratory animals available. American Physiological Society. Physiologist 39(4):199, 208–211.

Bhowmick S, D'Mello V, Abdul-Muneer PM (2019) Synergistic inhibition of ERK1/2 and JNK, not p38, phosphorylation ameliorates neuronal damages after traumatic brain injury. Mol Neurobiol 56(2): 1124–1136. https://doi.org/10.1007/s12035-018-1132-7

Chang W, Tegang K, Samuels BA, Saxe M, Wichmann J, David DJ, David IM, Augustin A, Fischer H, Golling S, Lamerz J, Roth D, Graf M, Zoffmann S, Santarelli L, Jagasia R, Hen R (2024) Pharmacological enhancement of adult hippocampal neurogenesis improves behavioral pattern separation in young and aged mice. Biol Psychiatry Glob Open Sci 5(2): 100419. https://doi.org/10.1016/j.bpsgos.2024.100419

Chidambaram SB, Anand N, Varma SR, Ramamurthy S, Vichitra C, Sharma A, Mahalakshmi AM, Essa MM (2024) Superoxide dismutase and neurological disorders. IBRO Neurosci Rep 16: 373–394. https://doi.org/10.1016/j.ibneur.2023.11.007

Deng P, Tang N, Li L, Zou G, Xu Y, Liu Z (2022) Diagnostic value of combined detection of IL-1β, IL-6, and TNF-α for sepsis-induced cardiomyopathy. Med Clín (Engl Ed) 158(9): 413–417. https://doi.org/10.1016/j.medcle.2021.04.032

Ferrell CL (2015) Anaphylactic reaction to methylprednisolone. J Emerg Nurs 41(6): 470–473. https://doi.org/10.1016/j.jen.2015.06.010

Ilyas S, Midoen YH, Santoso P (2025) A novel therapeutic approach to doxorubicin-induced cardiotoxicity, with a particular emphasis on the potential cardioprotective properties of *Vitis gracilis* Wall. J Pharm Pharmacogn Res 13(1): 254–263. https://doi.org/10.56499/jppres24.2000_13.1.254

Ilyas S, Santoso P, Midoen YH, Situmorang PC (2023) Improvement of spermatozoa concentration due to maximal exercise with *Vitis gracilis* Wall. J Pharm Pharmacogn Res 11(5): 874–886. https://doi.org/10.56499/jppres23.1685_11.5.874

James SL, Bannick MS, Montjoy-Venning WC, Lucchesi LR, Dandona L, Dandona R, Hawley C, Hay SI, Jakovljevic M, Khalil I, Krohn KJ, Mokdad AH, Naghavi M, Nichols E, Reiner RC, Smith M, Feigin VL, Vos T, Murray CJL, Zaman SB (2019) Global, regional, and national burden of traumatic brain injury

and spinal cord injury, 1990-2016: A systematic analysis for the Global Burden of Disease study 2016. Lancet Neurol 18(1): 56–87. https://doi.org/10.1016/S1474-4422(18)30415-0

Jana K, Dutta A, Chakraborty P, Manna I, Firdaus SB, Bandyopadhyay D, Chattopadhyay R, Chakravarty B (2014) Alpha-lipoic acid and N-acetylcysteine protects intensive swimming exercise-mediated germ-cell depletion, pro-oxidant generation, and alteration of steroidogenesis in rat testis. Mol Reprod Dev 81(9): 833–850. https://doi.org/10.1002/mrd.22354

Jeon IH, Kim HS, Kang HJ, Lee HS, Jeong SI, Kim SJ, Jang SI (2014) Anti-inflammatory and antipruritic effects of luteolin from perilla (*Perilla frutescens* L.) leaves. Molecules 19(6): 6941–6951. https://doi.org/10.3390/molecules19066941

Keating CE, Cullen DK (2021) Mechanosensation in traumatic brain injury. Neurobiol Dis 148: 105210. https://doi.org/10.1016/j.nbd.2020.105210

Kurniawan VR, Islam AA, Adhimarta W, Zainuddin, AA, Widodo D, Nasrullah, Ihwan A, Wahyudi, Faruk M (2022) The role of diphenhydramine HCl on tumor necrosis factor-α levels in Wistar rats with traumatic brain injury: An *in vivo* study. Ann Med Surg 81: 104399. https://doi.org/10.1016/j.amsu.2022.104399

Majeed U, Shafi A, Majeed H, Akram K, Liu X, Ye J, Luo Y (2023) Grape (*Vitis vinifera* L.) phytochemicals and their biochemical protective mechanisms against leading pathologies. Food Chem 405(Part A): 134762. https://doi.org/10.1016/j.foodchem.2022.134762

Marbun AP, Suryanto D, Elimasni (2024) Phytochemical screening, antioxidant activity and antimicrobials activity of ethanol extract of gagatan harimau leaves (*Paraboea leuserensis* B.L Burtt). J Penelit Pendidik IPA 10(12): 10909–10916. https://doi.org/10.29303/jppipa.v10i12.8428

Mathiasen JR, Dicamillo A (2010) Novel object recognition in the rat: A facile assay for cognitive function. Curr Protoc Pharmacol 49: 5.59.1-5.59.15. https://doi.org/10.1002/0471141755.ph0559s49

Mehta J, Rolta R, Mehta BB, Kaushik N, Choi EH, Kaushik NK (2022) Role of dexamethasone and methylprednisolone corticosteroids in coronavirus disease 2019 hospitalized patients: A Review. Front Microbiol 13: 813358. https://doi.org/10.3389/fmicb.2022.813358

Midoen YH, Ilyas S, Santoso P, Situmorang PC (2023) Effect of maximal physical exercise on apoptosis via cytochrome c in hippocampus cells after administration of *Vitis gracilis* Wall. J Pharm Pharmacogn Res 11(2): 297–307. https://doi.org/10.56499/jppres22.1563_11.2.297

Mohammed FS, Omay SB, Sheth KN, Zhou J (2023) Nanoparticle-based drug delivery for the treatment of traumatic brain injury. Expert Opin Drug Deliv 20(1): 55–73. https://doi.org/10.1080/17425247.2023.2152001

Musi CA, Agrò G, Santarella F, Iervasi E, Borsello T (2020) JNK3 as therapeutic target and biomarker in neurodegenerative and neurodevelopmental brain diseases. Cells 9(10) 2190. https://doi.org/10.3390/cells9102190

Sai Kumar S, Rinku DR, Pradeep Kumar A, Maddula R, Anna Palagan C (2023) An IOT framework for detecting cardiac arrhythmias in real-time using deep learning resnet model. Meas Sens 29: 100866. https://doi.org/10.1016/j.measen.2023.100866

Seibenhener ML, Wooten MC (2015) Use of the open field maze to measure locomotor and anxiety-like behavior in mice. J Vis Exp 96: e52434. https://doi.org/10.3791/52434

Shahzad S, Ahmad S, Madiha S, Khaliq S, Liaquat L, Sadir S, Rafiq S, Tabassum S, Batool Z, Haider S (2017) Dizocilpine induced psychosis-like behavior in rats: A possible animal model with full spectrum of schizophrenia. Pakistan Journal of Pharmaceutical Sciences 30(6): 2423–2427.

Shen B, Zhang H, Zhu Z, Ling Z, Zeng F, Wang Y, Wang J (2023) Baicalin relieves LPS-induced lung inflammation via the NF-κB and MAPK pathways. Molecules 28(4): 1873. https://doi.org/10.3390/molecules28041873

Silvestro S, Mazzon E (2023) Nrf2 activation: Involvement in central nervous system traumatic injuries. A promising therapeutic target of natural compounds. Int J Mol Sci 24(1): 199. https://doi.org/10.3390/ijms24010199

Situmorang PC, Ilyas S, Hutahaean S, Rosidah R (2019) Effect of nanoherbal andaliman (*Zanthoxylum acanthopodium*) and extra virgin olive oil combination on preeclamptic rats liver histology. Open Access Maced J Med Sci 7(14): 2226–2231. https://doi.org/10.3889/oamjms.2019.651

Slomianka L, Amrein I, Knuesel I, Sørensen JC, Wolfer DP (2011) Hippocampal pyramidal cells: The reemergence of cortical lamination. Brain Struct Funct 216(4): 301–317. https://doi.org/10.1007/s00429-011-0322-0

Thanos PK, Restif C, O'Rourke JR, Lam CY, Metaxas D (2017) Mouse Social Interaction Test (MoST): A quantitative computer automated analysis of behavior. J Neural Transm 124(1): 3–11. https://doi.org/10.1007/s00702-015-1487-0

Wang X, Li Y, Han L, Li J, Liu C, Sun C (2021) Role of flavonoids in the treatment of iron overload. Front Cell Dev Biol 9: 685364. https://doi.org/10.3389/fcell.2021.685364

Wasnis NZ, Ilyas S, Hutahaean S, Silaban R, Situmorang PC (2022) Effect of *Vitis gracilis* Wall (gagatan harimau) in the recovery of gastrocnemius muscle cells and cytochrome c expression of *Mus musculus*. J Pharm Pharmacogn Res 10(2): 303–309. https://doi.org/10.56499/jppres21.1208_10.2.303

Wu AG, Yong YY, Pan YR, Zhang L, Wu JM, Zhang Y, Tang Y, Wei J, Yu L, Law BYK, Yu CL, Liu J, Lan C, Xu RX, Zhou XG, Qin DL (2022) Targeting Nrf2-mediated oxidative stress response in traumatic brain injury: Therapeutic perspectives of phytochemicals. Oxid Med Cell Longev 2023: 1015791. https://doi.org/10.1155/2022/1015791

Yusuf F, Ilyas S, Damanik HA, Fatchiyah F (2016) Microbiota composition, HSP70 and caspase-3 expression as marker for colorectal cancer patients in Aceh, Indonesia. Acta Med Indones 48(4): 289-299.

AUTHOR CONTRIBUTION:

Contribution	Ilyas S	Midoen YH	Safni
Concepts or ideas	x	x	
Design	x	x	
Definition of intellectual content	x		x
Literature search			x
Experimental studies			x
Data acquisition	x	x	
Data analysis	x	x	
Statistical analysis		x	
Manuscript preparation		x	x
Manuscript editing		x	
Manuscript review	x	x	x

Citation Format: Ilyas S, Midoen YH, Safni (2026) Neuroprotective effects of nanoformulated *Paraboea leuserensis* B.L.Burtt on memory loss and depression in traumatic brain injury–induced rats: Behavioral and molecular insights. J Pharm Pharmacogn Res 14(2): 2415. https://doi.org/10.56499/jppres_14.2.2415

Publisher's Note: All claims expressed in this article are solely those of the authors and do not necessarily represent those of their affiliated organizations, or those of the publisher, the editors and the reviewers. Any product that may be evaluated in this article, or claim that may be made by its manufacturer, is not guaranteed or endorsed by the publisher.

Open Access: This article is distributed under the terms of the Creative Commons Attribution 4.0 International License (http://creativecommons.org/ licenses/by/4.0/), which permits use, duplication, adaptation, distribution and reproduction in any medium or format, as long as you give appropriate credit to the original author(s) and the source, provide a link to the Creative Commons license and indicate if changes were made.